Design and Development of Novel Nanocomposite Materials and Reactor Systems for Photocatalysis

Jeremiah F. Wilson, Sammie Ely III, Bria M. Moore[†], Lamont Henderson, Sesha Srinivasan[*], P.C. Sharma[*]
Department of Physics, Tuskegee University, Tuskegee, AL 36088, USA
[*]Faculty Mentors, [†]Currently a Graduate Student at Duke University

Abstract

With the support from the Sigma Pi Sigma and SPS-AIP Undergraduate research award, the current project is successfully implemented and executed to develop both novel materials' and the home-made reactor for the decontamination of water based organics such as Methyl Orange via visible light photocatalysis. For the novel materials', we have successfully developed visible light activated photocatalyst by varying the concentrations of low band gap semiconductor oxide $InVO_4$ with high band gap TiO_2 anatase matrix. Extensive analytical characterizations have been carried out using SEM, FTIR and BET to explore the surface morphology, chemical, surface area and pore size distribution of these nanocomposites. The new materials' selection TiO_2-Xwt.%$InVO_4$ have shown enhancement in photocatalytic degradation (by at least 50%) of Methyl Orange (MO), an azo dye decontamination in DI H_2O under visible light irradiation only. The visible light photocatalytic degradation performance of either plain TiO_2 or plain $InVO_4$ seems inert under the same operating conditions used for the above nanocomposites.

Introduction

Purification of water from organic contaminants, disinfection of water and air [1-4], destruction of bacterial activity [5], non-polluting power generation (including solar energy) [6, 7], reduction or stabilization of CO_2 [8, 9] and photodegradation of deep horizon oil spill [10] are the vital areas of urban, economic, environmental and industrial developments in the United States. Success in all these areas strongly depends on the development of efficient, inexpensive, environmentally friendly and chemically stable catalysts and photocatalysts. Titanium dioxide (TiO_2) is widely used in many photocatalytic [11, 12] and water splitting [13, 14] applications because of its high stability, low cost, non toxic, high oxidation and reduction potential and chemically favorable properties. However, it can only utilize the ultraviolet portion of the solar spectrum which results in low total efficiency of such catalyst in the sunlight energy utilization. The relationship between the energy bandgap and wavelength/frequency of the solar spectrum is shown in Fig. 1. From this figure, in order to work in the visible light wavelength above 400 nm (e.g. 400 – 800 nm), the photocatalytic material to be developed should have at least energy band gap between ~1.6-2.9 eV. In other words, the color of the photocatalyst should be between blue and red as depicted in Fig. 1.

Any improvements in photocatalytic efficiency of TiO_2 or development of other novel and new generation photocatalysts towards shifting their activity to the visible portion of the solar spectrum will have a significant impact. Indium vanadium oxide or Indium Vanadate ($InVO_4$) is chosen as a viable photocatalyst with low band gap of 1.8-2.0 eV, and is demonstrated to split water and reduce CO_2 in to methanol, under visible light irradiation [15-18]. It has been demonstrated to couple both the wide bandgap TiO_2 and narrow bandgap $InVO_4$ semiconductors, so that it can facilitate for better charge carriers separation (see Fig. 2 for band edge positions for both TiO_2 and $InVO_4$). In addition to the novel materials' development, it is also proposed to design custom made reactor for the UV-visible light photocatalysis for the photo-oxidation of toxic organics in aqueous based samples. In Fig. 2, $InVO_4$ has its conduction band positioned above TiO_2's. $InVO_4$'s valence band is positioned above the oxidation potential

for the hydroxide ion, and thus, hydroxyl radicals cannot be formed with $InVO_4$. The purpose of coupling $InVO_4$ and TiO_2 is to exploit the higher conduction band of $InVO_4$ as a way to separate charge. If electrons are sequestered in the $InVO_4$, they cannot recombine with h_{vb}^+ in TiO_2. The respective crystal structure of both anatase TiO_2 and $InVO_4$ are given in the insets of Fig. 2.

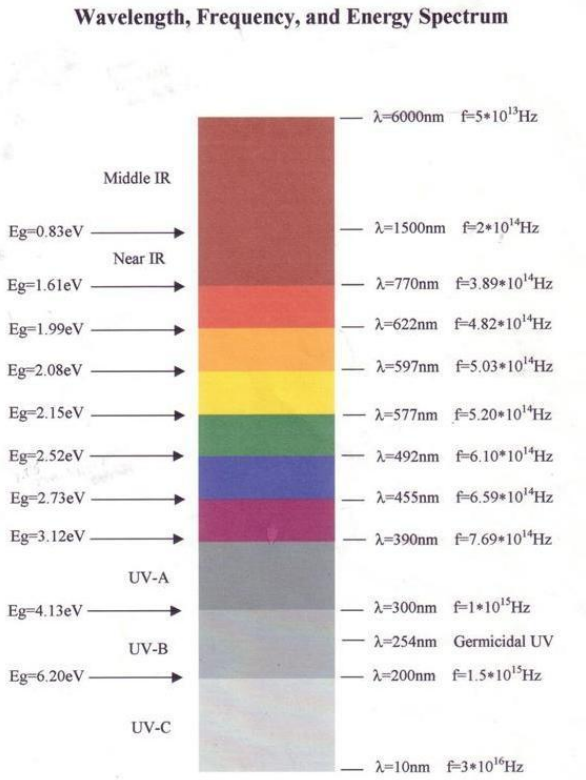

Fig. 1: Solar energy spectrum – relation of wavelength, frequency and band gap

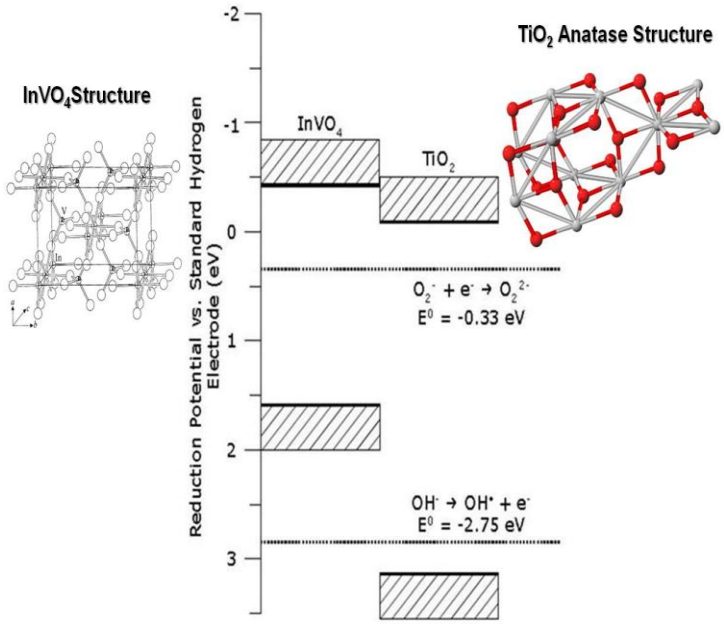

Fig. 2: Band edge diagram of TiO_2 (Eg ~ 3.2 eV) and $InVO_4$ (Eg ~ 2eV)

Experimental Details

The TiO_2-Xwt% $InVO_4$ nanocomposites are synthesized by both wet chemical route and solid state mechanochemical process as discussed below and also depicted in flow chart of Fig. 3.

Chemical Synthesis of $InVO_4$: From literature we learned that it is possible to chemically synthesize $InVO_4$ from a precursor made by reacting $In(OH)_3$ and V_2O_5 under heat with a multi-dentate ligand such as diethyenetriaminepentaacetic acid (DTPA). The first attempt of calcinating the precursor material in a tubular furnace was not successful as it produced charred product. Alternatively, the precursors were treated in a muffle furnace and this leads to produce the desired $InVO_4$. This change produced promising results as far as similar characteristics to the standard $InVO_4$. We have tried a variety of different methods or strategies within the process in order to obtain a higher yield of the product; such as (i) muffle furnace vs. stove top drying of precursor, (ii) slow ramping of temp vs. quickly increasing temp during precursor formation, (iii) increase in initial mass of compounds etc. The above experimental parameters have been tailored for the optimum yield of $InVO_4$ in a single step synthesis process.

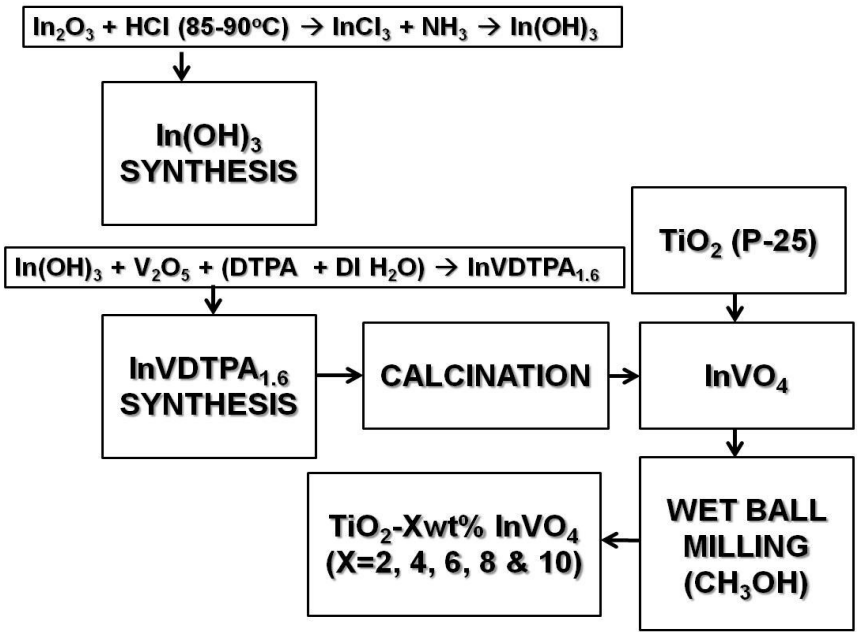

Fig. 3: Flow chart synthesis of $InVO_4$ and TiO_2-Xwt% $InVO_4$

Mechano-chemical Synthesis of TiO_2-Xwt% $InVO_4$: Wet mechanochemical milling was employed for the synthesis of nanocomposites of TiO_2 with different concentrations of $InVO_4$. Methyl alcohol (at least 5ml) was used as a medium of wet milling about one hour duration. The chemical concentration of $InVO_4$ was varied like, 2, 4, 6, 8 and 10 in terms of weight basis and ad-mixed with TiO_2. The other experimental parameters such as ball to power ratio, forward and reverse milling conditions etc. have been optimized for the high yield of the composite nanoparticles. It is visually seen from the ball milled powder, which turns to dark blue (or pale blue) from plain white color of TiO_2 and brown or (pale brown) color of $InVO_4$. Thus the obtained nanocomposites are further subjected to metrological and photocatalytic characterizations.

Analytical Characterization of TiO_2-Xwt% $InVO_4$: The as-synthesized nanocomposites have been subjected to chemical, microstructural and surface area analysis characterizations using

FTIR (Shimadzu), Scanning Electron Microscope (Zeiss Instrument) and BET nitrogen physisorption (Quantachrome's Autosorb iQ) tools.

Photo-oxidation of methyl orange (azo dye) using TiO_2-Xwt% $InVO_4$: The nanocomposite materials are used for testing in our home-made photocatalytic reactor for the degradation of methyl orange (MO) in aqueous water under visible light and UV-visible light conditions (see Fig. 4 below). Various parameters such as air purging, catalyst concentration pollutant (MO) concentration in at least 1000 ml of DI H_2O, sampling interval, pH variations which degradation of chemical etc. This photocatalytic water oxidation method was adopted to validate the nature and concentration of nanocomposites needed for the optimum performance under only visible light irradiations. Thus obtained results were compared with the photocatalytic characteristics of plain TiO_2 and plain $InVO_4$ under same experimental conditions. UV spectrometer (Shimadzu) was used to analyze the absorption concentration of Mo after centrifuging the sampling vials. UVProbe software was used to analyze the obtained data to calculate the rate.

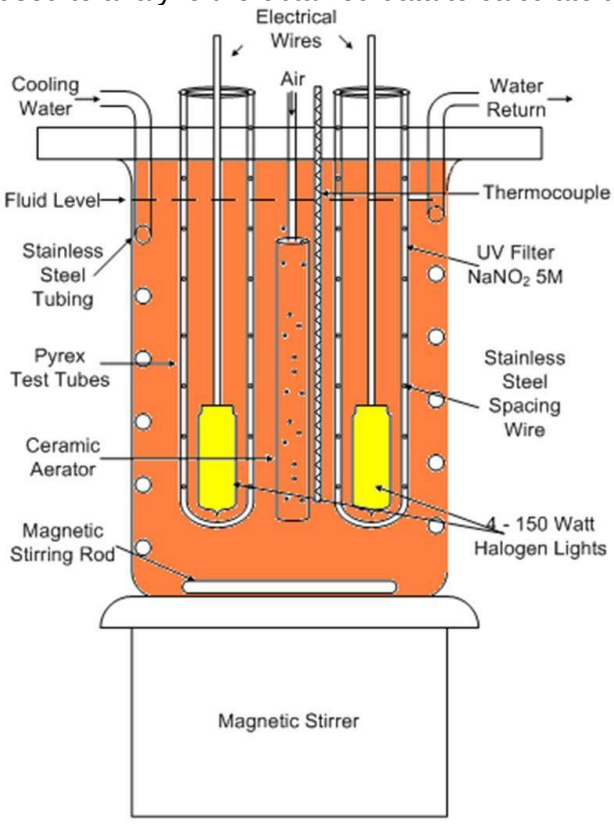

Fig. 4: Schematic diagram for the design of photocatalytic batch reactor for the degradation of MO in 1000ml of aqueous water under UV-Visible light.

Results and Discussion

The $InVO_4$ samples synthesized by different processes such as using tubular furnace, hot plate and muffle furnace are shown in Fig. 5(a). From this figure, it is very well understood the by using tubular furnace, due to the temperature gradient, the color of the product turned black. However, under appropriate experimental conditions using muffle furnace calcinations yielded the pale brown or brown color sample which were further subjected to analytical characterizations. For the mechanochemical milled nanocomposites of TiO_2-Xwt.%$InVO_4$, the product material turned to blue color (or pale blue) and these samples neither inherited the white color of TiO_2 nor the brown color of the $InVO_4$ (see Fig. 5(b)).

Fig. 5(a): $InVO_4$ synthesized via chemical route using heat treated precursors

Fig. 5(b): TiO_2-X%$InVO_4$ (X=2, 4, 6, 8, 10) sample synthesized via wet-milling.

Fourier Transform Infrared spectra for the plain TiO_2, plain $InVO_4$ and TiO_2-Xwt% $InVO_4$ (X=2, 4, 6, 8, 10) have been recorded using Shimadzu FTIR spectrometer. Table 1 shows the indexing of the bonding stretches and bending modes of C-H, C-N, V-O, V-O-V, V-O-In, $InVO_4$ vibrations at respective wavenumber. From the FTIR profiles (not shown a graph here), it is noticed that the composite nanoparticles of TiO_2 with increasing concentrations of $InVO_4$ thus enhances the bonding bands at the order of at least 10 cm^{-1}.

Table 1: Fourier Transform Infrared Spectra bonding information of TiO_2-Xwt% $InVO_4$

Wavenumber, cm^{-1}	Chemical Bonding Information
448.6	V-O-V
767.4; 903.5	V-O-In
943.7	V-O
3415.4	InVO4
2925; 2851	C-H Stretches
1420	C-N Stretch

BET surface area analysis (nitrogen physisorption at 77K) of the TiO_2-Xwt% $InVO_4$ have been carried out under liquid nitrogen temperature using Autosorb iQ equipment and are also compared with the plain TiO_2 and pristine $InVO_4$. Fig. 6 shows the variation of surface area with respect to different samples mentioned above. It is noteworthy to mention 4%$InVO_4$ ad-mixed with TiO_2 shows at least 1.5 times more surface area (~92 m^2/g) than plain TiO_2 (~63 m^2/g).

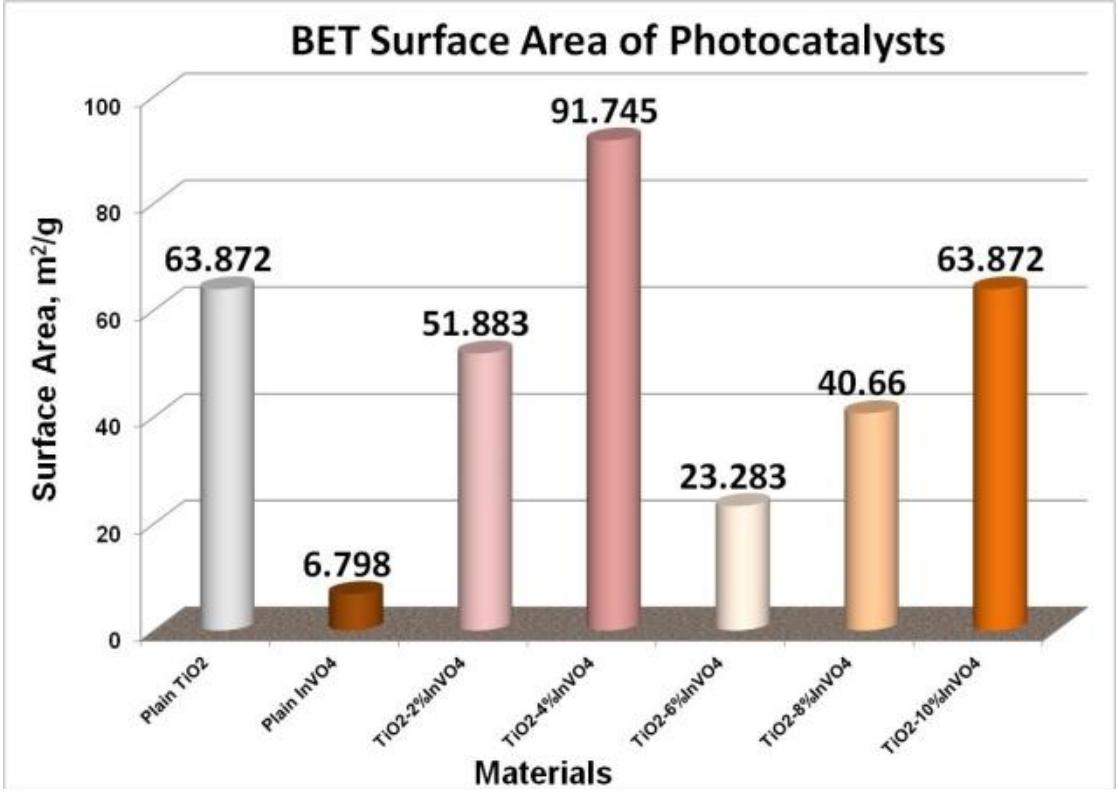

Fig. 6: BET surface area for the plain and $InVO_4$ doped TiO_2 nanoparticles.

The pore size distribution data such as pore volume and average pore size of the plain and $InVO_4$ doped TiO_2 are tabulated in Table 2. The average pore size of the nanocomposites is obviously higher than either the plain TiO_2 or plain $InVO_4$.

Table 2: BET surface area analysis of plain TiO_2, $InVO_4$ and TiO_2-Xwt% $InVO_4$

SAMPLE	S.AREA	PORE VOL	AVE. PORE
	m^2/g	cc/g	SIZE nm
$InVO_4$	6.798	0.003	1.82
2%$InVO_4$	51.883	0.025	1.944
4%$InVO_4$	91.745	0.044	1.922
6%$InVO_4$	23.283	0.011	1.95
8%$InVO_4$	40.66	0.020	1.938
10%$InVO_4$	47.303	0.023	1.955
TiO_2	63.872	0.030	1.881

Scanning electron micrographs of the plain TiO_2, plain $InVO_4$ and TiO_2-4%$InVO_4$ have been obtained from Zeiss Instrument. The morphology of plain TiO_2 shows spongy white color, whereas the $InVO_4$ shows more porous structure (see Fig. 7(a) and 7(b)). For the TiO_2/$InVO_4$ nanocomposite structure, it exhibits heritance of neither TiO_2 nor $InVO_4$ morphology. However it does shows uniform sandwich of the two compounds in molecular level (Fig. 7(c)).

Photocatalytic water detoxification and air disinfection under the solar irradiation is considered and recognized to be an environmental sustainable technology. Titanium oxide (TiO_2) nanoparticles have demonstrated greater efficiency in degrading water borne chemicals such as phenol, azo-dyes (methyl orange, methylene blue etc.) under UV radiation. This is due to their high band gap of TiO_2 which is approximately 3.2 eV. The presence of UV (λ<400 nm) in the entire solar spectrum is only 4%, and rest of 96% contribution is due to the visible light (λ=400-800 nm). $InVO_4$ was chosen for the coupling, since they possess lower energy gap (~2eV) with appropriate energy levels with respect to TiO_2, in order to facilitate longer separation of generated electron and hole carriers for potential mineralization of organic contaminants under visible light. In this project, we have developed coupled semiconductor oxide nanoparticles (TiO_2-Xwt.% $InVO_4$) using chemical and mechanochemical routes discussed in the previous section.

The increase in the surface area of the TiO_2/$InVO_4$ nanocomposite as shown in Fig. 6 above will enhance the photocatalytic behavior since the photo-oxidation of MO is apparently a surface phenomenon. The photocatalytic oxidation experiments have been conducted using the plain TiO_2, plain $InVO_4$ and TiO_2-Xwt% $InVO_4$ under UV-Visible irradiation of MO/DI H_2O for different time durations. Plain TiO_2 under UV light demonstrated higher activity of degrading MO in at least 5 hours due to its intrinsic photocatalytic behavior (Fig. 8(a)).

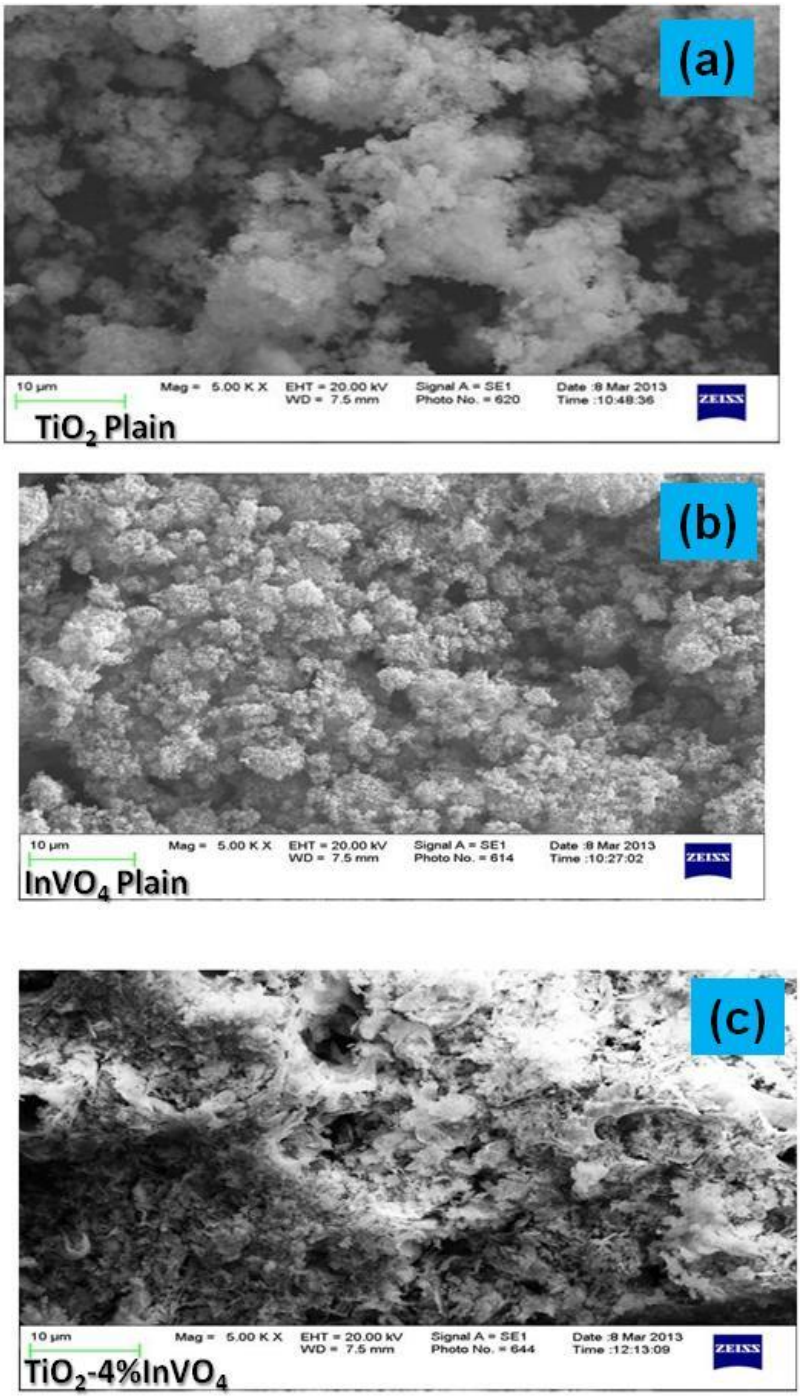

Fig. 7: SEM microstructures of plain TiO_2, plain $InVO_4$ and TiO_2-Xwt% $InVO_4$

On the other hand, plain $InVO_4$ was inert towards the photo-oxidation reaction and discoloration was noticed over 7 hours of light exposure (Fig. 8(b)). For the TiO_2-4wt% $InVO_4$ samples, the degradation of 80% of MO was systematically occurred in 7 hours (Fig. 8(c)), however, the kinetics of this degradation reaction needs to be improved. The degradation of MO concentration (C) with its original concentration (C_0) was recorded with respect to the total time for the degradation reaction is plotted in Fig. 9. Again this degradation of 80% in 7 hours of

duration is due to the UV-Visible light source combination, however the project participants continued their progress to show the effect of degradation only using visible light which is the scope of the further study given below.

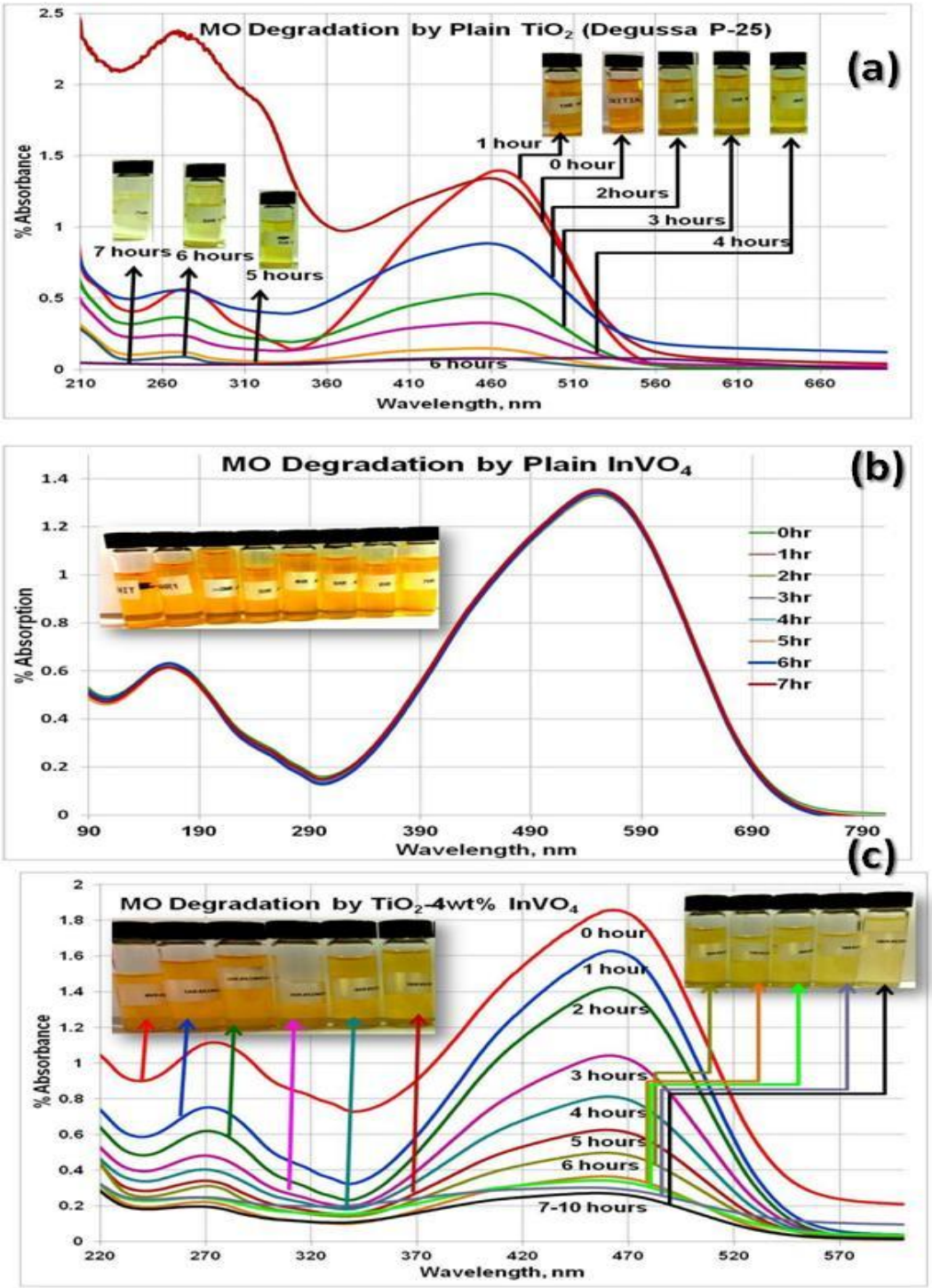

Fig. 8: Photo-oxidation of 20 ppm of MO in aqueous water using photocatalysts.

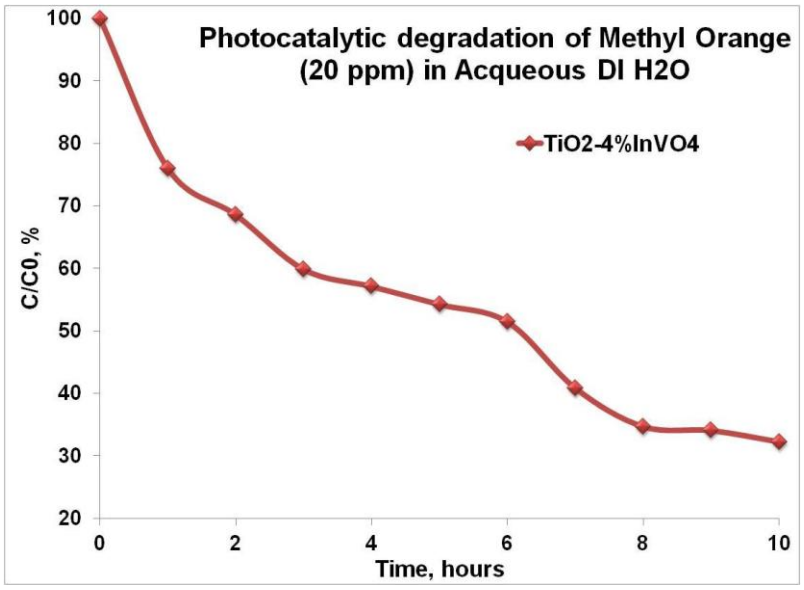

Fig. 9: MO concentration degradation of TiO2-4%InVO4 using UV-Visible light.

Fig. 10 below represents the photocatalytic degradation of methyl orange (MO) using both plain TiO_2 and various concentrations of $InVO_4$ ad-mixed TiO_2 under visible light only. The UV component of the light source was cut-off by an Edmund Optics UV cut-off filter, so the t wavelength above 400 nm was only allowed to reach the catalyst suspended MO/DI water solution. $InVO_4$ concentration less than 4% demonstrated higher photo-oxidation to degrade MO at least 50% in 120 minutes. The UV absorption characteristic peak of MO at ~450 nm degrades with different time interval is shown in the inset of Fig. 10. It is unambiguously clear that having the ad-mixture of $InVO_4$ in a critical composition is highly effective under visible light while maintaining the catalytic property of TiO_2.

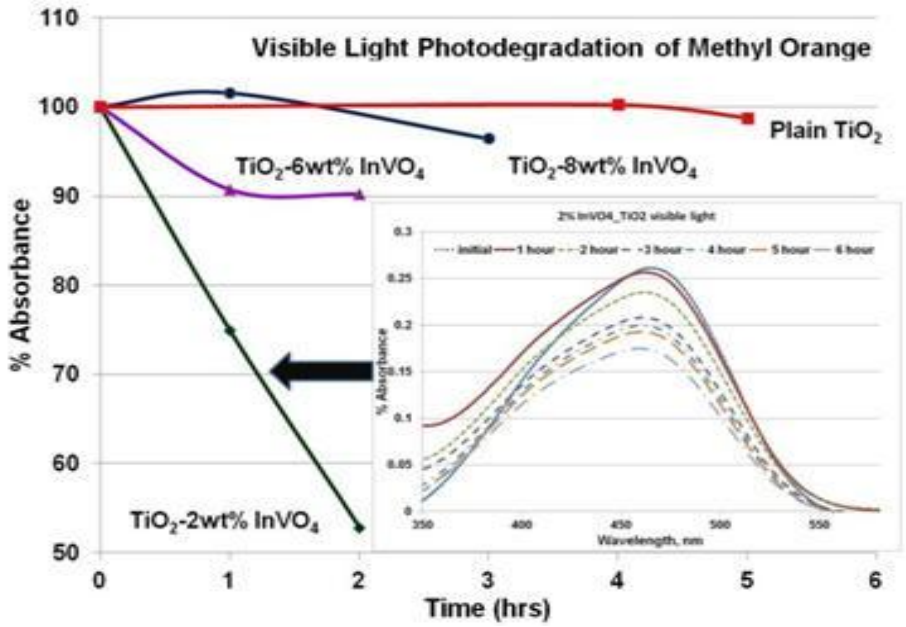

Fig. 10: Photocatalytic degradation of Methyl Orange in DI H_2O for plain TiO_2 and TiO_2-Xwt.%$InVO_4$ (X=2, 6, 8) under visible light irradiation

Conclusion

In summary, the preliminary results showed that the new catalysts TiO_2-Xwt% $InVO_4$ are promising in water purification applications due to their higher surface area in comparison to either plain TiO_2 or plain $InVO_4$. Another important aspect of this research study is that this experimental research work has successfully incorporated in our Modern Physics Laboratory course. Students enrolled in this course will routinely trained to work on the state-of-the-art research tools such as FTIR, UV-Vis spectrometers, High Energy Ball Mill, Photocatalytic batch reactors, Autosorb iQ surface area tool and RGA/MS etc.

Future Work

The following statement of works (in bullets) are proposed to improve both materials' and engineering design aspects related to this project to generate hydrocarbon fuel from photocatalytic reduction of CO_2 and H_2O.

- Mechanochemical preparation of nano Ni (0.1-1 mole concentrations) doped TiO_2-Xwt.%$InVO_4$ using high energy planetary ball mill.
- Thermochemical preparation of atomic nitrogen doped TiO_2-Xwt.%$InVO_4$ using ammoniation route using tubular programmable furnace.
- Surface area analysis and other physico-chemical characterizations (FTIR, XRD, SEM, and EDAX) of newly prepared materials (mentioned in above two bullets).
- Photocatalytic degradation testing of the modified photocatalyst under plain UV, plain visible light and combination of UV-Visible light irradiations.
- Photocatalytic fuel reactor design and its optimization to maximize the hydrocarbon or alcohol production using feed mixtures of CO_2 and H_2O vapor.
- Energy efficiency, rate of reaction, and cost effectiveness calculations for the scale-up of lab reactor design to the commercial stand point.

Financial Budgetary Expenditures

Item #	Item Description	Amount (in US $)
1	Fume hood annual safety certification by SafetyPlus LLC	280.00
2	¼ inch stainless steel caps for PARR reactor – 4 quantities	70.00
3	300 psi gauge + gas hose with check valve assembly	750.00
4	SEM characterization – Auburn University user facility	600.00
5	Chemicals + Solvents + Acids + Bases + Surfactants	300.00
	Total	**2000.00**

Acknowledgements

Financial support from Sigma Pi Sigma, American Institute of Physics (AIP-SPS Undergraduate Research Award) is gratefully acknowledged.

References

1. C. P. Huang, C. Dong and Z. Tang, Advanced chemical oxidation: Its present role and potential future in hazardous waste treatment, Waste Management, 13 (2003) 361.
2. A. Mills, R.H. Davies and D. Wosley, Water-purification by semiconductor photocatalysis, Chem. Soc. Rev., 1993, 417
3. M.R. Hoffman, S.T. Martin, W. Choi and D.W. Bahnemann, Environmental Applications of Semiconductor Photocatalysis, Chem. Rev., 95 (1995) 69
4. W.A. Jacoby, D.M. Blake, J.A. Fennell, J.E. Bouleter, L.M. Vargo, MC. George and S.K. Dolber, J. Air and Waste Management Association, 46, Sept. (1996)
5. P. Maness, S. Smolinski, D.M. Blake, Z. Huang, E.J. Wolfrum and W.A. Jacoby, Bactericidal Activity of Photocatalytic TiO_2 Reaction: toward an Understanding of Its Killing Mechanism, App. and Env. Microbiology, Sept. 1999, 4094
6. B. Viswanathan, Photocatalytic processes – Selection Criteria for the Choice of Materials, Bull. Catal. Soc. India, 2 (2003) 71
7. T-V. Nguyen, H-C. Lee, O.-B. Yang, The effect of pre-thermal treatment of TiO_2 nano-particles on the performances of dye-sensitized solar cells, Solar Energy Materials & Solar Cells, 90, 7-8 (2006) 967-981.
8. H. Yamashita, Y. Fujii, Y. Ichihashi, S.G, Zhang, K. Ikeue, D.R, Park, K. Koyano, T, Tatsumi and M. Anpo, Selective Formation of CH3OH in the Photocatalytic Reduction of CO_2 with H_2O on Titantium Oxide Highly dispersed within Zeolites and Mesoporous Molecular Sieves, Catal. Today, 45 (1998) 221
9. K. Ikeue, H. Yamashita and M. Anpo, Photocatalytic reduction of CO2 with H2O on titanium oxides prepared within the FSM-16 mesoporous zeolite, Chem. Lett., (1999) 1135
10. M.J. García-Martínez, I.D. Riva, L. Canoira, J.F. Llamas, R. Alcántara and J.L.R. Gallego, Photodegradation of polycyclic aromatic hydrocarbons in fossil fuels catalyzed by supported TiO_2, Applied Catalysis B: Environmental 67, 3-4, (2006) 279-289.
11. K. Rajeshwar, C.R. Chenthamarakshan, S. Georinger and M. Djukic, Titania-based heterogeneous photocatalysis. Materials, mechanistic issues, and implications for environmental remediation, Pure Appl. Chem., 73, 12 (2001) 1849.
12. A. Wold, Photocatalytic properties of TiO_2, Chem. Mater, 5 (1993) 280-283.
13. A. Fujishima and K. Honda, Nature, Electrochemical Photolysis of Water at a Semiconductor Electrode, 238 (1972) 37
14. M. Ni, M-K.H Leung, D-Y.C. Leung and K. Sumathy, A review and recent developments in photocatalytic water-splitting using TiO_2 for hydrogen production, Renewable and Sustainable Energy Reviews, 11 (2007) 401
15. N. Serpone and E. Pelizzetti, Photocatalysis: Fundamentals and Applications, JohnWiley & Sons, New York, NY, USA, 1989.
16. M. A. Fox and M. T. Dulay, “Heterogeneous photocatalysis,” Chemical Reviews, vol. 93, no. 1, pp. 341–357, 1993.
17. N. Kislov, S.S. Srinivasan, Yu. Emirov, E.K. Stefanakos, Optical absorption red and blue shifts in $ZnFe_2O_4$ nanoparticles, Materials Science and Engineering B, 153 (2008) 70-77.
18. K.M Tarquinio, N.K Kothurkar, D.Y Goswami, R.C Sanders Jr, A.L Zaritsky, A.M. LeVine, Bactericidal effects of silver plus titanium dioxide-coated endotracheal tubes on *Pseudomonas aeruginosa* and *Staphylococcus aureus*, International Journal of Nanomedicine, 5 (2010) 177–183.